Cancer "-omics"

Molecular Cancer Research

Comparative Genomics Reveals Shared Mutational Landscape in Canine Hemangiosarcoma and Human Angiosarcoma

Kate Megquier[1,2], Jason Turner-Maier[1], Ross Swofford[1], Jong-Hyuk Kim[3,4,5], Aaron L. Sarver[4,5,6], Chao Wang[2], Sharadha Sakthikumar[1,2], Jeremy Johnson[1], Michele Koltookian[1], Mitzi Lewellen[3,4,5], Milcah C. Scott[3,4,5], Ashley J. Schulte[3,4,5], Luke Borst[7], Noriko Tonomura[1,8], Jessica Alfoldi[1], Corrie Painter[1,9], Rachael Thomas[10], Elinor K. Karlsson[1,11,12], Matthew Breen[10], Jaime F. Modiano[3,4,5,13,14,15,16], Ingegerd Elvers[1,2], and Kerstin Lindblad-Toh[1,2]

Abstract

Angiosarcoma is a highly aggressive cancer of blood vessel–forming cells with few effective treatment options and high patient mortality. It is both rare and heterogenous, making large, well-powered genomic studies nearly impossible. Dogs commonly suffer from a similar cancer, called hemangiosarcoma, with breeds like the golden retriever carrying heritable genetic factors that put them at high risk. If the clinical similarity of canine hemangiosarcoma and human angiosarcoma reflects shared genomic etiology, dogs could be a critically needed model for advancing angiosarcoma research. We assessed the genomic landscape of canine hemangiosarcoma via whole-exome sequencing (47 golden retriever hemangiosarcomas) and RNA sequencing (74 hemangiosarcomas from multiple breeds). Somatic coding mutations occurred most frequently in the tumor suppressor *TP53* (59.6% of cases) as well as two genes in the PI3K pathway: the oncogene *PIK3CA* (29.8%) and its regulatory subunit *PIK3R1* (8.5%). The predominant mutational signature was the age-associated deamination of cytosine to thymine. As reported in human angiosarcoma, *CDKN2A/B* was recurrently deleted and *VEGFA, KDR*, and *KIT* recurrently gained. We compared the canine data to human data recently released by The Angiosarcoma Project, and found many of the same genes and pathways significantly enriched for somatic mutations, particularly in breast and visceral angiosarcomas. Canine hemangiosarcoma closely models the genomic landscape of human angiosarcoma of the breast and viscera, and is a powerful tool for investigating the pathogenesis of this devastating disease.

Implications: We characterize the genomic landscape of canine hemangiosarcoma and demonstrate its similarity to human angiosarcoma.

Introduction

Angiosarcoma is an aggressive cancer of blood vessel–forming cells, associated with poor survival times (1–3). There is an unmet need for new diagnostics and therapies for these patients. However, the rarity of this cancer (approximately 0.01% of all cancers; refs. 4, 5) has limited large-scale genomic studies so far. Canine hemangiosarcoma is a relevant clinical model for understanding the pathophysiology of human angiosarcoma. The human and canine diseases share many clinical similarities, and hemangiosarcoma is common in dogs, occurring in some breeds (notably the golden retriever) with a frequency up to 20% (6). This means that using canine hemangiosarcoma as a model for human disease would yield sample cohorts of a magnitude inaccessible using human data alone. However, for dogs to be an effective

[1]Broad Institute of Harvard and MIT, Cambridge, Massachusetts. [2]Science for Life Laboratory, Department of Medical Biochemistry and Microbiology, Uppsala University, Uppsala, Sweden. [3]Department of Veterinary Clinical Sciences, College of Veterinary Medicine, University of Minnesota, St. Paul, Minnesota. [4]Animal Cancer Care and Research Program, University of Minnesota, St. Paul, Minnesota. [5]Masonic Cancer Center, University of Minnesota, Minneapolis, Minnesota. [6]Institute for Health Informatics, University of Minnesota, Minneapolis, Minnesota. [7]Department of Clinical Sciences, North Carolina State College of Veterinary Medicine, Raleigh, North Carolina. [8]Tufts Cummings School of Veterinary Medicine, North Grafton, Massachusetts. [9]Count Me In, Cambridge, Massachusetts. [10]Department of Molecular Biomedical Sciences, North Carolina State University College of Veterinary Medicine, and Comparative Medicine Institute, Raleigh, North Carolina. [11]Program in Bioinformatics and Integrative Biology, University of Massachusetts Medical School, Worcester, Massachusetts. [12]Program in Molecular Medicine, University of Massachusetts Medical School, Worcester, Massachusetts. [13]Center for Immunology, University of Minnesota, Minneapolis, Minneapolis. [14]Stem Cell Institute, University of Minnesota, Minneapolis, Minnesota. [15]Institute for Engineering in Medicine, University of Minnesota, Minneapolis, Minnesota. [16]Department of Laboratory Medicine and Pathology, School of Medicine, University of Minnesota, Minneapolis, Minnesota.

Note: Supplementary data for this article are available at Molecular Cancer Research Online (http://mcr.aacrjournals.org/).

M. Breen, J.F. Modiano, I. Elvers, and K. Lindblad-Toh contributed equally to this article.

Corresponding Authors: Kate Megquier, Broad Institute of Harvard and MIT, 415 Main St., 75A-6108B, Cambridge, MA 02142. Phone: 617-714-8919; E-mail: kmegq@broadinstitute.org; and Kerstin Lindblad-Toh, kersli@broadinstitute.org

Mol Cancer Res 2019;17:2410–21

doi: 10.1158/1541-7786.MCR-19-0221

AACR

model of this disease in the era of precision medicine, detailed genomic characterization of canine hemangiosarcoma must be undertaken, and the results directly compared with existing and emerging genomic data from human angiosarcoma.

Angiosarcoma can form anywhere in the vasculature. In human patients, it most commonly occurs in the skin of the head, neck, and scalp, the breast, the extremities, and less frequently in the liver, right auricle of the heart, bone, and spleen (7). Prognosis is poor, with metastatic disease occurring in approximately 50% of cases (8), and a median overall survival time of approximately 50 months for local disease and 10 months in metastatic cases (9). Treatment involves surgical resection with wide margins, plus or minus radiotherapy, as well as adjuvant chemotherapy in the metastatic disease setting (3). Many angiosarcomas are initially sensitive to doxorubicin, paclitaxel, or targeted agents, but resistance to these therapies is virtually inevitable (3).

While most cases of angiosarcoma in humans occur without known cause, there are several known risk factors. These tumors can arise secondary to radiotherapy for other cancers or chronic lymphedema (3). Other known risk factors include UV irradiation, given the typical locations of cutaneous angiosarcomas on the head and neck (10–12), as well as occupational exposure to vinyl chloride (13), arsenic exposure (14), and use of anabolic steroids (15). Genetically, angiosarcoma is associated with familial syndromes including Li-Fraumeni syndrome (*TP53* mutations; ref. 16) and Klippel–Trenaunay syndrome (*PIK3CA* mutations; ref. 17). However, these syndromes do not solely cause angiosarcoma (7), and angiosarcomas are not present in the majority of cases.

Canine hemangiosarcoma is the histopathologic equivalent of human angiosarcoma (18), and follows a similar, aggressive clinical course. In dogs, the most common tumor locations are the spleen, right auricle of the heart, liver, and skin or subcutaneous tissue (19, 20). The different anatomic distribution seen in the human and canine diseases is likely due, at least in part, to the lack of secondary cases in dogs. Treatment protocols for dogs with hemangiosarcoma similarly involve wide surgical resection, followed by adjuvant chemotherapy. Survival times are short—a median of 4–6 months after surgical resection with adjuvant chemotherapy, with a 1-year survival rate of approximately 10% (21–23). Biological risk factors have not yet been identified in dogs. Genetically, dog breeds display differential predisposition to specific cancers, indicating that there are heritable risk factors that have become common as a result of inbreeding based on selection or drift. In a previous genome-wide association study, we identified several loci significantly associated with the risk of hemangiosarcoma in the golden retriever (24).

Recent targeted next-generation sequencing of human angiosarcomas has begun to reveal the somatic mutational spectrum of this disease. It has so far proven to be fairly heterogeneous—no pathognomonic mutations or copy number aberrations occur in all cases, and tumors from different primary locations or with different underlying etiologies have genomic differences. *TP53* and genes in the MAPK pathway are frequently mutated (25), and mutations in *PLCG1* and *PTPRB* are common, particularly in secondary angiosarcomas (25, 26). Although the PI3K pathway is activated in some human angiosarcomas (27, 28), *PIK3CA* mutations have so far not been commonly reported in human angiosarcoma studies (26, 29). Genes in the VEGF pathway are frequently gained or amplified, including *VEGFA* and *KDR* (25, 28). The tumor suppressor *CDKN2A* is frequently deleted, while the *MYC* oncogene is frequently amplified, most commonly in radiation-associated tumors (25, 28).

In dogs, a recent whole-exome sequencing (WES) study of a small cohort of 20 hemangiosarcomas showed that the top recurrently mutated genes were *PIK3CA* and *TP53* (30). Earlier candidate gene studies of canine hemangiosarcomas reported mutations in *TP53* (31), *PTEN* (32), and *PDGFRA* and *PDGFRB* (33). An analysis of somatic copy number aberrations in visceral hemangiosarcomas from five breeds found that *VEGFA* was recurrently gained, while *CDKN2A* was frequently deleted (34). *MYC* copy number gain was infrequent, likely reflective of the fact that secondary hemangiosarcomas are not seen in canine patients (34). While these earlier studies provide clues as to the genetic features of canine hemangiosarcoma, there is very little of the genome-wide data needed for comprehensive comparison with human angiosarcoma.

To assess the potential utility of hemangiosarcoma as a model for angiosarcoma at the molecular level, we performed the largest exome-sequencing study of hemangiosarcoma to date, and complemented our exome data with oligonucleotide array comparative genomic hybridization (oaCGH) copy number data and RNA-sequencing (RNA-seq) data in partially overlapping cohorts of hemangiosarcoma cases. We then performed comparative analyses of our results with those released by The Angiosarcoma Project direct-to-patient initiative. In this way, we have created a detailed genomic profile of this cancer in the golden retriever breed, and begun vetting this canine cancer as a comparative model for human angiosarcoma, and potentially other tumors.

Materials and Methods

Additional Materials and Methods can be found in the Supplementary Materials and Methods, and a workflow in Supplementary Fig. S1.

Canine hemangiosarcoma sample collection for exome sequencing

Samples were obtained as part of necessary diagnostic procedures with owner consent. DNA from tumor tissue and whole blood was collected from 47 golden retrievers with visceral hemangiosarcoma. Samples were collected from dogs referred for treatment at the University of Minnesota (UMN) Veterinary Medical Center and samples submitted to the Modiano laboratory for diagnostic assessment and/or use in research (n = 34), from cases seen at the North Carolina State University (NCSU) Veterinary Hospital (n = 8), or from diagnostic samples sent to Antech Diagnostics (n = 5). Cases where date of diagnosis was known (n = 36), were diagnosed between 2000 and 2014. Tumor samples were either frozen (n = 17), or formalin-fixed, paraffin-embedded (n = 30; Supplementary Table S1). Procedures involving animal use were approved by the Institutional Animal Care and Use Committees at the Broad Institute (Cambridge, MA), UMN (Minneapolis, MN), or NCSU (Raleigh, NC).

Sample preparation

DNA was extracted and sequencing libraries prepared using the Kapa Hyper Prep Kit (Supplementary Table S2). For 66 samples, additional cycles of PCR were required to obtain sufficient DNA for exome capture, while libraries from 28 samples were

reconstructed from source DNA using the standard protocol (see Supplementary Information).

Exome capture

The Roche Nimblegen SeqCap-EZ capture canine exome (120705_CF3_Uppsala_Broad_EZ_HX1) was used for hybrid exome capture, following the manufacturer's protocol.

Sequencing and read alignments

The barcoded exome-captured libraries were multiplexed in pools of eight, and sequenced on the Illumina HiSeq 2500 to a target depth of 60× in the tumor and 30× in the normal, reaching a mean depth of 78× in the tumor and 63× in the normal. Reads were aligned to the CanFam3.1 reference genome using BWA. PCR duplicate reads were flagged using the Picard tool MarkDuplicates. Following the Genome Analysis Toolkit (GATK) Best Practices, we then performed Base Quality Score Recalibration using a set of approximately 19 million known canine germline variant locations.

Somatic variant calling

Somatic mutations were called using MuTect2, using the default settings with the addition of the *dontUseSoftClippedBases* option, which was added to avoid calling a large number of artifactual indels in our FFPE-preserved samples (see Supplementary Methods). To further refine our set of somatic variant calls, and to avoid artifacts, we also called variants using the GATK4 version of Mutect2, and kept only the consensus of calls which passed in both the GATK3 and GATK4 versions. Both sets of calls were filtered using a "panel of normals" created using all 47 normal (germline) samples, as well as germline samples from previous studies of canine lymphoma, osteosarcoma, and melanoma. Calls were further filtered to exclude oxidation artifacts, and were removed if they overlapped locations with known germline variants. Variants were further filtered if the position had low coverage (defined as a read depth less than 20 in the normal, less than 40 in the tumor, or less than four alternate allele reads in the tumor) or had excessive read depth (greater or equal to mean read depth + 5× SD), to filter out potential alignment errors. Finally, variants with a median read position < 10 were filtered to remove potential artifacts.

Variant annotation

Variants were annotated using the variant effect prediction program SnpEff v4.2. Where multiple effects were predicted for a single variant, the most damaging predicted effect was selected. Coding variants were analyzed using the *smg* function in Genome MuSiC 0.4 to determine which genes were significantly mutated above the background rate. The *merge-concurrent-muts* option was applied to count multiple mutations in the same gene within a sample as a single mutation, and a FDR threshold of 0.1 using the convolution test (CT) was applied.

Canine mutational signature discovery

Mutational signatures, considering point mutations and their genomic context, were extracted using a Bayesian nonnegative matrix factorization (NMF) algorithm. The discovered signatures were compared with known signatures in COSMIC (35), as well as those reported in the literature for human angiosarcoma (36). The overall landscape of mutations was plotted for different groupings of samples using the SomaticSignatures package.

RNA sequencing of canine hemangiosarcomas

Seventy-four snap-frozen samples were obtained from 73 dogs with hemangiosarcoma (41 golden retrievers and 32 dogs from 13 other breeds or from mixed breeding; Kim and colleagues, manuscript in preparation). RNA-seq data from 51 of the hemangiosarcoma tissues had been published previously (37, 38). RNA-seq libraries were generated as described previously (37).

Somatic copy number detection in canine hemangiosarcomas

Analysis of somatic copy number aberrations (SCNA) in our canine WES data was limited by the inclusion of both frozen and formalin-fixed samples. The FFPE samples appeared to have an increased number of amplifications and deletions when compared with the frozen samples, possibly as a result of DNA fragmentation during the fixation process (39). While we were able to partially account for this using correction for guanine and cytosine content (40), we were not able to completely remove the bias between the two groups (Supplementary Fig. S6). Hence, we instead used oaCGH data to interrogate copy number changes in a cohort of 69 golden retrievers with hemangiosarcoma tumors, of which 28 were also included in the exome sequencing cohort. SCNAs were called from oligonucleotide array comparative genomic hybridization (oaCGH), as described previously (34), using a approximately 180,000-feature microarray (Agilent Technologies) with approximately 26 kb resolution throughout the dog genome.

Accessing human data from The Angiosarcoma Project for comparative analysis

We compared the somatic mutations and SCNAs present in our cohort of canine hemangiosarcomas to the results reported by The Angiosarcoma Project, a direct-to-patient sequencing project run by the Count Me In initiative (JoinCountMeIn.org). Somatic mutations and SCNAs derived from WES data from 48 samples from 36 patients were downloaded from cBioPortal, and somatic mutations classified as nonsense, missense, splice site, or splice region were kept for analysis. For our analysis, we selected only the annotated primary tumor site from each patient, including 30 tumors—17 breast, five visceral (one each of right atrium, spleen, lung, abdomen, and bladder wall), and eight head, face, neck, and scalp (HFNS) tumors.

Pathway analysis in canine and human data

Pathway analysis was performed on the canine and human mutational data using the DAVID Functional Annotation Tool. For the overall enrichment analyses, all genes with nonsynonymous splice site, or splice region somatic mutations were used. Functional annotation charts were created for Kyoto Encyclopedia of Genes and Genomes (KEGG) pathways using the default options, using the Benjamini–Hochberg method to control the FDR. Analysis was performed independently for the canine data and the human data, mapping genes from both species to *Homo sapiens* reference to avoid confounding due to differences in gene annotation between the species. Canine Ensembl gene IDs were mapped to their 1:1 orthologs in the human GRCh37 reference genome annotation using Ensembl's BioMart (41).

Data availability

The WES data, as well as the RNA-seq data that has not been previously published, has been submitted to the NCBI Sequence Read Archive. WES data: BioProject PRJNA552034, BioSamples SAMN12173468 - SAMN12173561. RNA-seq data:

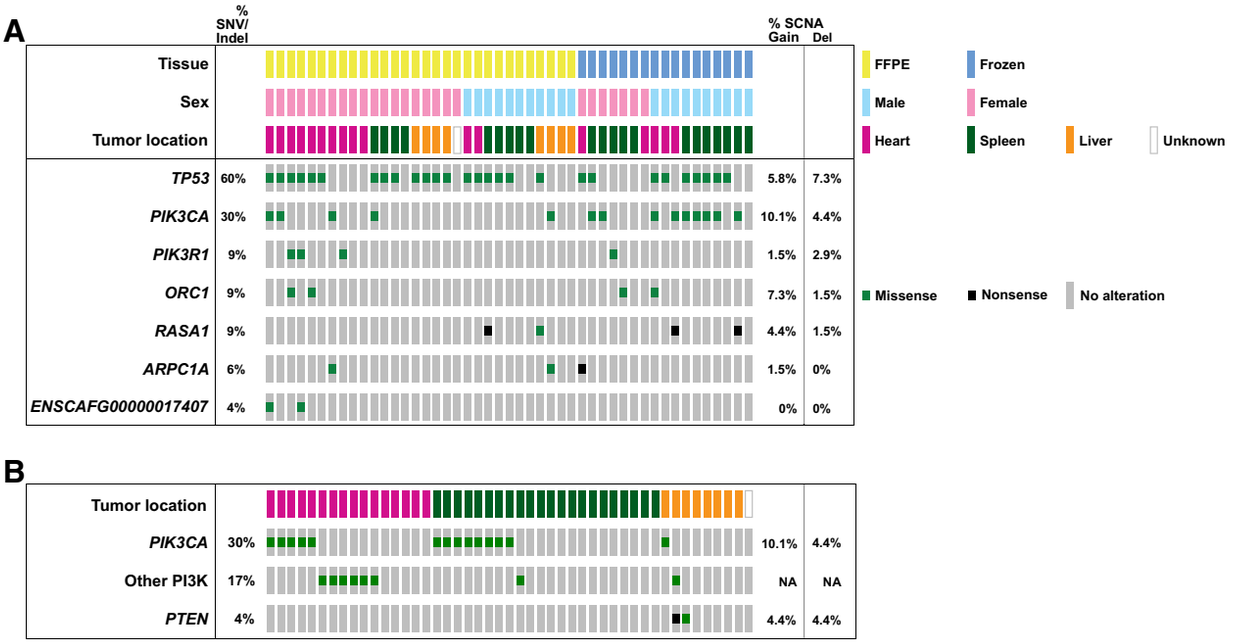

Figure 1.
Per-sample annotation of metadata. **A,** Somatic mutations in the seven significantly mutated genes. **B,** Somatic mutations in the *PI3K* gene family by tumor location. "Other PI3K" category includes mutations in *PIK3CB, PIK3C2G, PIK3C3, PIK3R1*, and *PIK3R5*). SNV, single-nucleotide variant; Indel, insertion/deletion; SCNA, somatic copy number aberration. SCNA frequencies are calculated on the basis of oaCGH data from 69 canine hemangiosarcoma samples.

BioProject PRJNA562916, BioSamples SAMN12659339 - SAMN12659361.

Results

Simple somatic mutations

TP53 and PIK3CA are commonly mutated in canine hemangiosarcomas. The seven significantly mutated genes (SMGs) in the canine hemangiosarcomas contained well-known cancer genes, including *TP53*, as well as two genes in the PI3K pathway (Table 1; Fig. 1). Tumor suppressor *TP53* was most frequently mutated (28/47 cases, 59.6%), with all 28 cases carrying at least one mutation affecting the DNA-binding domain (Fig. 2). Oncogene *PIK3CA* (14/47, 29.8%) and its regulatory subunit *PIK3R1* (4/47, 8.5%) were both mutated. Ten of the 14 cases with *PIK3CA* mutations had a mutation at amino acid position 1047, a hotspot frequently mutated in many types of human cancers (ref. 42; Fig. 2). The remaining four SMGs were *ORC1* (4/47, 8.5%), *RASA1* (4/47, 8.5%), *ARPC1A* (3/47, 6.4%), and *ENSCAFG00000017407* (2/47, 4.3%), a "one-to-many" ortholog of human *ATP5PD* with 27 paralogs in the canine genome. Overall, 59 genes that were mutated at least once in the canine dataset are annotated as having likely causal somatic mutations in the COSMIC Cancer Gene Census (43), including *TP53, PIK3CA*, and *PIK3R1* (Supplementary Table S3).

Variant allele fraction and effect predictions. For further insight into whether the four SMGs not annotated in COSMIC are likely to be driver mutations, we investigated the variant allele fraction (VAF) of each and whether missense mutations were predicted to be deleterious or tolerated using the SIFT (44) score via Ensembl's Variant Effect Predictor (45). The median VAF for the four *RASA1*

Table 1. Significantly mutated genes in golden retriever hemangiosarcoma tumors

Gene ID	Gene name	Indels	SNVs	Total mutations	Covd Bps	Muts pMbp	*P*	FDR
TP53	Tumor protein p53	3	25	28	72,582	386	0	0
PIK3CA	Phosphatidylinositol-4,5-bisphosphate 3-kinase catalytic subunit alpha	0	14	14	156,415	90	0	0
PIK3R1	Phosphoinositide-3-kinase regulatory subunit 1	0	4	4	124,857	32	7.3×10^{-8}	5.9×10^{-4}
ORC1	Origin recognition complex subunit 1	0	4	4	133,219	30	1.3×10^{-7}	8.2×10^{-4}
RASA1	RAS p21 protein activator 1	0	4	4	136,539	29	3.2×10^{-6}	1.6×10^{-2}
ARPC1A	Actin-related protein 2/3 complex subunit 1A	0	3	3	72,351	41	1.3×10^{-5}	5.1×10^{-2}
ENSCAFG00000017407	1-to-many ortholog of human ATP synthase peripheral stalk subunit d (*ATP5PD*)	0	2	2	22,074	91	1.7×10^{-5}	5.9×10^{-2}

NOTE: Significantly mutated genes with an FDR < 0.1, calculated using Genome MuSiC.
Abbreviations: Covd Bps, number of basepairs with adequate coverage in gene; SNV, single nucleotide variants; Muts pMbp, mutations per megabase.

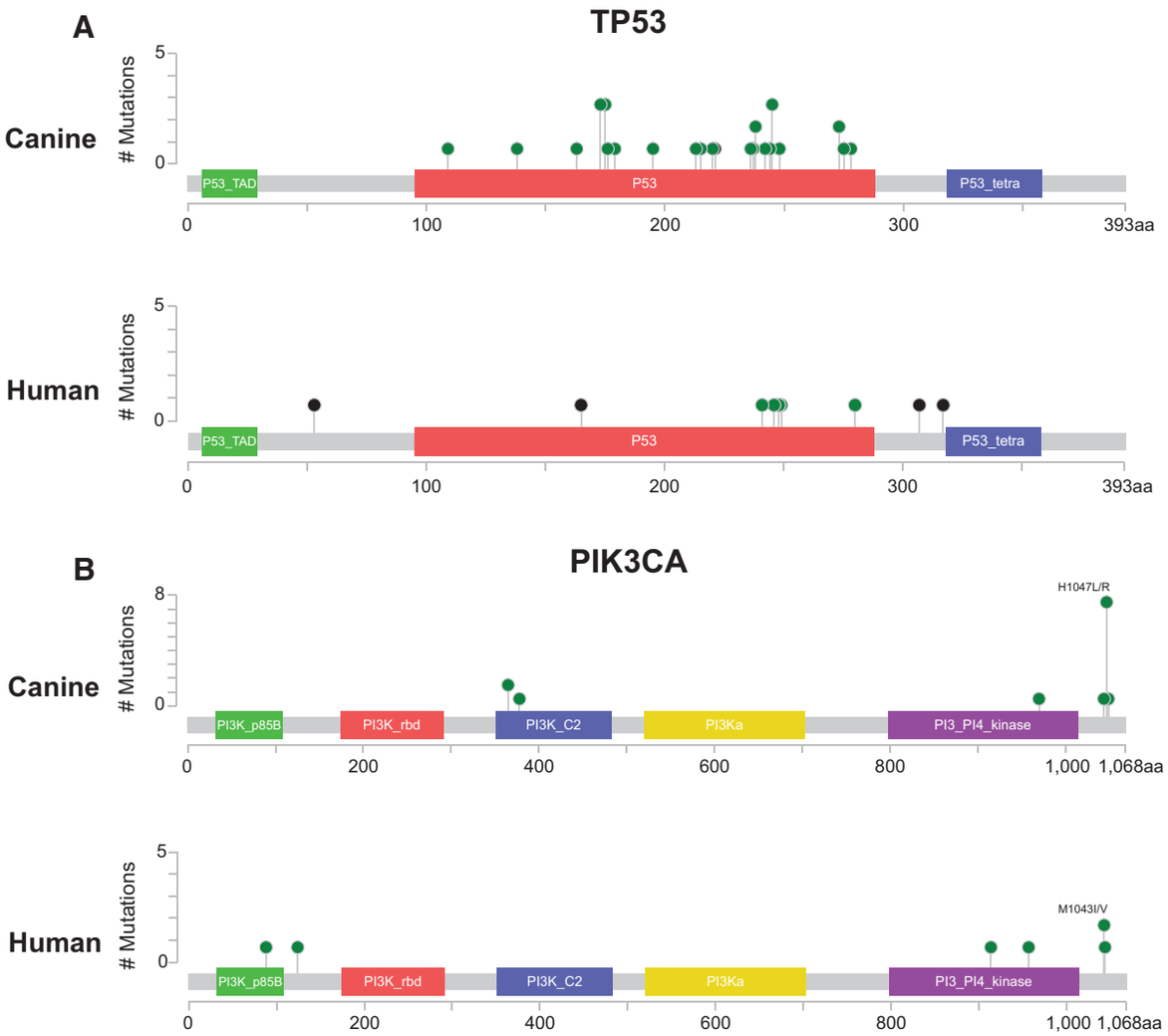

Figure 2.

Lollipop plots showing the positions of the tumor protein p53 (TP53; **A**) and phosphatidylinositol-4,5-bisphosphate 3-kinase catalytic subunit alpha (PIK3CA; **B**) mutations in the canine and human data. Canine mutational locations were lifted over to the human hg19 reference genome using the LiftOver tool. Green, missense mutation; Black, truncating mutation.

mutations was 0.12 (range 0.08–0.23). Three mutations were nonsense mutations, with the fourth a missense mutation predicted to be deleterious (SIFT score 0), supporting a causal role for these mutations. Similarly, the median VAF of the three *ARPC1A* mutations was 0.16 (range 0.12–0.17), with one nonsense mutation, and two missense mutations at the same position, predicted to be deleterious (SIFT score 0). The median VAF for the four *ORC1* mutations (all at the same position) was lower, at 0.08, and the change was predicted to be tolerated (SIFT score 0.06). The two mutations in *ENSCAFG00000017407* also had a low median VAF (0.05), and were predicted to be tolerated (SIFT score 1).

Comparison with top mutated genes in human angiosarcoma. The most commonly mutated genes in the human data were *TP53* (8/30 tumors, 29%), followed by *KDR*, *LRP2*, *RYR2*, and *ABCA13* with mutations in 7 of 30 tumors each, and *PIK3CA*, *FLG*, *ASXL3*, *MYH14*, and *UNC13C*, mutated in 6 of 30 tumors each. However, the distribution of these mutations varied by tumor location. In the human data, breast tumors were the only location to carry *PIK3CA* mutations ($n = 6$ patients), and were the most common location for *KDR* mutations. *TP53* mutations occurred in all locations, but were more common in HFNS and visceral tumors. *KDR* was much less frequently mutated in the canine cohort, with only one case having a nonsynonymous mutation, predicted to be tolerated. Two human tumors also had mutations in the canine SMG *RASA1*. One was a nonsense mutation, the other predicted to be deleterious.

Differential patterns of mutations found in some tumor locations. The pattern of mutations in the PI3K gene family varied by tumor location in the canine data, as well. In the canine cases, a slightly higher proportion of heart tumors (11/16, 68.8%) compared with splenic tumors (9/22, 40.9%) had PI3K alterations, although this

Table 2. KEGG pathways enriched in hemangiosarcoma, visceral and breast angiosarcoma, and HFNS angiosarcoma

Angiosarcoma - visceral and breast		Hemangiosarcoma		Angiosarcoma - HFNS	
Term	***P***	**Term**	***P***	**Term**	***P***
hsa04020:Calcium signaling pathway	5.4E-03	hsa05200:Pathways in cancer	3.6E-04	hsa02010:ABC transporters	2.5E-08
hsa04730:Long-term depression	7.1E-03	hsa04360:Axon guidance	3.8E-04	hsa04510:Focal adhesion	8.1E-04
hsa04015:Rap1 signaling pathway	9.0E-03	hsa04919:Thyroid hormone signaling pathway	5.9E-04	hsa04512:ECM-receptor interaction	9.6E-04
hsa04510:Focal adhesion	2.2E-02	hsa04664:Fc epsilon RI signaling pathway	6.7E-04	hsa04740:Olfactory transduction	1.1E-03
hsa04720:Long-term potentiation	2.2E-02	hsa04510:Focal adhesion	1.4E-03	hsa04724:Glutamatergic synapse	1.3E-03
hsa04010:MAPK signaling pathway	2.3E-02	hsa05146:Amoebiasis	1.4E-03	hsa04974:Protein digestion and absorption	2.9E-03
hsa05230:Central carbon metabolism in cancer	2.3E-02	hsa05214:Glioma	1.5E-03	hsa04611:Platelet activation	3.8E-03
hsa05200:Pathways in cancer	4.8E-02	hsa05215:Prostate cancer	1.5E-03	hsa04610:Complement and coagulation cascades	8.1E-03
		hsa04070:Phosphatidylinositol signaling system	1.7E-03	hsa04976:Bile secretion	8.1E-03
		hsa05230:Central carbon metabolism in cancer	3.0E-03	hsa04730:Long-term depression	8.6E-03
		hsa05223:Non-small cell lung cancer	3.4E-03	hsa04713:Circadian entrainment	8.7E-03
		hsa05221:Acute myeloid leukemia	3.4E-03	hsa04723:Retrograde endocannabinoid signaling	9.5E-03
		hsa04750:Inflammatory mediator regulation of TRP channels	3.8E-03	hsa04022:cGMP-PKG signaling pathway	1.8E-02
		hsa04012:ErbB signaling pathway	3.9E-03	hsa05033:Nicotine addiction	1.9E-02
		hsa04015:Rap1 signaling pathway	5.8E-03	hsa04020:Calcium signaling pathway	1.9E-02
		hsa05213:Endometrial cancer	5.9E-03	hsa04024:cAMP signaling pathway	2.9E-02
		hsa04151:PI3K-Akt signaling pathway	1.2E-02	hsa05146:Amoebiasis	3.4E-02
		hsa05231:Choline metabolism in cancer	1.3E-02	hsa04151:PI3K-Akt signaling pathway	4.1E-02
		hsa04014:Ras signaling pathway	1.3E-02	hsa04080:Neuroactive ligand-receptor interaction	4.4E-02
		hsa04730:Long-term depression	1.5E-02	hsa05205:Proteoglycans in cancer	4.6E-02
		hsa00562:Inositol phosphate metabolism	1.5E-02	hsa04925:Aldosterone synthesis and secretion	4.8E-02
		hsa04370:VEGF signaling pathway	1.6E-02		
		hsa04713:Circadian entrainment	1.7E-02		
		hsa05222:Small cell lung cancer	1.9E-02		
		hsa04725:Cholinergic synapse	2.2E-02		
		hsa04915:Estrogen signaling pathway	2.3E-02		
		hsa04723:Retrograde endocannabinoid signaling	2.5E-02		
		hsa04724:Glutamatergic synapse	2.6E-02		
		hsa04020:Calcium signaling pathway	2.8E-02		
		hsa04662:B cell receptor signaling pathway	2.9E-02		
		hsa04611:Platelet activation	3.1E-02		
		hsa05218:Melanoma	3.3E-02		
		hsa04917:Prolactin signaling pathway	3.3E-02		
		hsa05220:Chronic myeloid leukemia	3.6E-02		
		hsa05205:Proteoglycans in cancer	3.7E-02		
		hsa04921:Oxytocin signaling pathway	4.5E-02		

NOTE: Blue, pathways enriched in both visceral and breast angiosarcoma and hemangiosarcoma; yellow, pathways enriched in both HFNS angiosarcoma and hemangiosarcoma; green, pathways enriched in all three groups.

Table 3. Overlap of mutated genes between canine hemangiosarcoma and human angiosarcoma tumors in several gene families and pathways

Gene family	Human only	Shared	Canine only
Phosphatidylinositol signaling system KEGG pathway	*DGKB, DGKD, DGKQ, IMPA2, INPP4B, ITPR1, ITPR2, ITPR3, PI4KA, PIK3CG, PIK3R2, PIP5K1B, PLCB1, PRKCB*	*DGKI, PIK3C2G,* ***PIK3CA****, PLCB2, PLCB3, PLCG1, PLCG2, PTEN*	*DGKG, PIK3C3, PIK3CB,* ***PIK3R1****, PIK3R5, PLCB4, PLCE1*
Phospholipase C	*PLCB1, PLCH1, PLCXD1, PLCXD3*	*PLCB2, PLCB3, PLCG1, PLCG2*	*PLCB4, PLCE1*
Protein tyrosine phosphatase	*PTP4A2, PTPN7, PTPN9, PTPN13, PTPN23, PTPRA, PTPRB, PTPRC, PTPRH, PTPRO, PTPRQ, PTPRR, PTPRS, PTPRT*	*PTPN5, PTPN22, PTPRD, PTPRJ, PTPRK, PTPRZ1*	*PTP4A1, PTPDC1, PTPN4*
LDL receptor-related proteins	*LRP3*	*LRP1, LRP1B, LRP2, LRP4*	
Histone methyltransferase/ demethylase activity GO terms	*EHMT2, KDM4A, KDM4B, KDM4D, KDM5C, KDM6B, KMT2B, KMT2C, NSD1, PHF2, PRDM16, PRDM7, PRDM9, SETD2, SETDB1, SETDB2*	*KDM5A, KMT2D, MECOM*	*JMJD1C, KDM3A, KMT2A, PRMT2*
MAPK signaling pathway KEGG pathway	*AKT3, ARRB1, CACNA1A, CACNA1B, CACNA1G, CACNA1I, CACNA1S, CACNA2D1, CACNA2D2, CACNA2D3, CACNB1, CACNB3, CACNG3, CHP2, CHUK, DUSP4, EGF, FGF7, FGF12, FGFR2, FLNC, GRB2, HRAS, HSPA1L, MAP2K3, MAP3K4, MAP3K5, MAP3K11, MAP4K1, MAP4K3, MAP4K4, MAPK10, MAPK8IP3, MOS, MYC, NF1, NTRK1, NTRK2, PAK2, PDGFRA, PDGFRB, PPP3CA, PRKCB, PTPN7, PTPRR, RAF1, RAPGEF2, RASGRF2, RASGRP3, RPS6KA1, RPS6KA5, RPS6KA6, TAOK1, TGFB2*	*BRAF, CACNA1D, CACNA1E, CACNA1H, CACNB2, FGFR3, MECOM, NRAS, PLA2G4A, PTPN5,* ***RASA1****, SOS2,* ***TP53***	*CACNA1C, IL1B, MAP3K6, MAP3K13, NFATC4, PLA2G4E, PPM1B, RASGRF1, RASGRP1, RPS6KA3, SOS1, STK4*
Protein tyrosine kinase activity GO terms	*ALK, BLK, CLK2, CLK3, DDR1, DDR2, DSTYK, EGF, EPHA2, EPHA3, EPHA4, EPHA6, EPHB4, EPHB6, ERBB2, ERBB3, FGF7, FGFR2, FLT4, FRK, HSP90AA1, KIT, MAP2K3, MATK, MERTK, NTRK1, NTRK2, PDGFRA, PDGFRB, PKDCC, PTK2B, RET, ROR2, ROS1, SGK223, SRMS, STYK1, SYK, TEC, TTK, TYRO3, ZAP70*	*EPHA5, EPHA7, ERBB4, FGFR3, FLT3, IGF1R, JAK1, KDR, NTRK3, PTK2, TIE1, TTN*	*CDC37, EFNB3, EPHB2, FYN, IL3RA, NRG1, NRP1, STAT5A, TEK, TYK2*

NOTE: Significantly mutated genes bolded.

difference was not significant ($P_{\chi}^{2} = 0.09$). Liver tumors had slightly fewer overall alterations in the *PI3K* gene family (3/8, 37.5%), and were less likely to have *PIK3CA* mutations (1/8, 12.5%), although this was not statistically significant.

Comparison of mutational burden by tumor location in canine and human data. We found fewer nonsynonymous and splice site/region mutations in the canine tumors than reported in the human tumors overall, while the number of mutations per sample varied significantly by tumor location in human cases. In the canine cohort, there were a median of 23 nonsynonymous coding mutations per sample (range 1–152; Supplementary Table S1), which was closest to the human breast (median = 32, $n = 17$), and visceral (median = 40, $n = 5$) tumors. In the dogs, there was a small difference in the total number of nonsynonymous and splice site/region mutations between heart (median = 31, $n = 15$, outlier with 152 mutations removed) and splenic ($n = 22$, median = 17.5) tumors ($P_{\text{TukeyHSD}} = 0.04$). In the human data, there was a significant difference in the median number of mutations by tumor location, with head, face, neck, and scalp (HFNS, $n = 8$) tumors having a higher mutational burden (median = 596.5) than breast or visceral tumors ($P_{\text{ANOVA}} = 3.6 \times 10^{-5}$; ref. 46).

Comparative pathway analysis highlights similarity between canine and human tumors. We compared the gene functional annotations enriched in hemangiosarcoma to those enriched in breast and visceral angiosarcoma and those enriched in HFNS angiosarcoma (Table 2). KEGG pathways enriched in canine hemangiosarcoma overlapped with KEGG pathways enriched in both subtypes of angiosarcoma. Pathways enriched in hemangiosarcoma included a larger fraction of those enriched in visceral and breast angiosarcoma (75%, vs. 48% of pathways enriched in HFNS angiosarcoma); however, the total number of pathways shared was greater between hemangiosarcoma and HFNS angiosarcoma (10 pathways). Pathways shared between hemangiosarcoma and visceral and breast angiosarcoma included pathways in cancer ($P_{\text{canine}} = 3.6 \times 10^{-4}$, $P_{\text{visceral/breast}} = 4.8 \times 10^{-2}$), Rap1 signaling pathway ($P_{\text{canine}} = 5.8 \times 10^{-3}$, $P_{\text{visceral/breast}} = 9.0 \times 10^{-3}$) and central carbon metabolism in cancer ($P_{\text{canine}} = 3.0 \times 10^{-3}$, $P_{\text{visceral/breast}} = 2.3 \times 10^{-2}$). Pathways shared between hemangiosarcoma, visceral and breast angiosarcoma, and HFNS angiosarcoma included focal adhesion pathway ($P_{\text{canine}} = 1.4 \times 10^{-3}$, $P_{\text{visceral/breast}} = 2.2 \times 10^{-2}$, $P_{\text{HFNS}} = 8.1 \times 10^{-4}$), calcium signaling pathway ($P_{\text{canine}} = 2.8 \times 10^{-2}$, $P_{\text{visceral/breast}} = 5.4 \times 10^{-3}$, $P_{\text{HFNS}} = 1.9 \times 10^{-2}$), and long-term depression ($P_{\text{canine}} = 1.5 \times 10^{-2}$, $P_{\text{visceral/breast}} = 7.1 \times 10^{-3}$, $P_{\text{HFNS}} = 8.6 \times 10^{-3}$).

In addition, functional annotation enrichment analysis of the genes mutated in hemangiosarcoma, visceral and breast angiosarcoma, and HFNS angiosarcoma found that they were enriched in many of the same protein domains. Shared domains include Fibronectin type III ($P_{\text{canine}} = 9.5 \times 10^{-9}$, $P_{\text{visceral/breast}} = 6.3 \times 10^{-5}$, $P_{\text{HFNS}} = 3.0 \times 10^{-15}$), Epidermal growth factor-like domain ($P_{\text{canine}} = 1.5 \times 10^{-3}$, $P_{\text{visceral/breast}} = 5.6 \times 10^{-5}$, $P_{\text{HFNS}} = 4.0 \times 10^{-16}$), and Tyrosine protein kinase active site ($P_{\text{canine}} = 6.9 \times 10^{-4}$, $P_{\text{visceral/breast}} = 3.8 \times 10^{-3}$, $P_{\text{HFNS}} = 2.3 \times 10^{-6}$). Both visceral and breast and HFNS angiosarcomas were enriched in cadherins ($P_{\text{visceral/breast}} = 4.9 \times 10^{-4}$, $P_{\text{HFNS}} = 4.7 \times 10^{-16}$), HFNS highly so, while hemangiosarcoma was not ($P_{\text{canine}} = 0.14$). In addition, HFNS angiosarcoma was enriched in ABC-transporters ($P = 2.8 \times 10^{-7}$) while visceral and breast angiosarcoma and canine hemangiosarcoma were not (Supplementary Table S7).

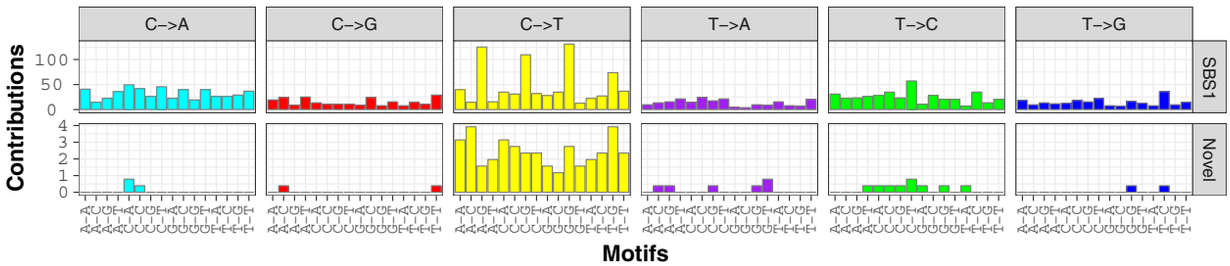

Figure 3.

Mutational signatures called using Bayesian NMF in the entire canine hemangiosarcoma cohort, showing the count of mutations (*y*-axis) in each trinucleotide context (*x*-axis). This analysis reveals the COSMIC SBS1 aging signature (top) and a faint novel signature (bottom).

Pathways and gene families previously reported in the angiosarcoma literature. Several pathways and gene families have been previously reported to be affected in the human angiosarcoma literature. Mutations in both *PLCG1* and *PTPRB* have been reported to be recurrent (26), particularly in secondary angiosarcoma. In the human data, 12 patients had mutations in eight phospholipase C genes, including *PLCG1* ($n = 5$, Table 3). Seven canine cases (15%) had mutations in PLC genes, including one in *PLCG1*. Twenty protein tyrosine phosphatases were mutated in 12 samples in human, including 2 patients with *PTPRB* mutations. While none of the canine tumors had somatic mutations in *PTPRB*, 8 cases (17%) harbored a mutation in one of nine other protein tyrosine phosphatase genes (Table 3).

The MAPK pathway has been reported to be frequently affected by mutations in angiosarcoma (25), and we found the visceral and breast angiosarcomas to be enriched in mutations in MAPK pathway genes ($P = 0.02$, Table 2). We noted mutations in 25 genes in the MAPK pathway in the canine cohort, including the SMGs *TP53* and *RASA1*. In the human data, 67 genes in the MAPK pathway were mutated. Thirteen of these genes were mutated in both the canine and human data (Table 3). Although we found mutations in genes involved in histone methyltransferase/demethylase activity in both species, consistent with earlier human studies (47), we saw no significant enrichment on a pathway level in either the canine or human cohorts (Table 3). Tyrosine protein kinases were enriched in both hemangiosarcoma and angiosarcoma. In the human data, 55 genes in the GO Protein Tyrosine Kinase Activity pathway were mutated, while 22 genes in this pathway were mutated in the canine data, with 12 genes mutated in both human and canine samples (Table 3). Low-density lipoprotein receptors were enriched for mutations in the canine ($P = 0.03$) and human HFNS tumors ($P = 0.05$), and *LRP2* was one of the most frequently mutated genes in the human dataset (mutated in 7/30 tumors). While mutations in the LDL receptor–related protein family have not been widely reported in human angiosarcoma, they have recently been shown to play a role in a variety of cancers (48). We found that four LDL receptor–related protein genes were mutated in both hemangiosarcoma and angiosarcoma, with an additional gene mutated in angiosarcoma only (Table 3).

Mutational signature of aging is present across all canine tumors. Analysis of mutational signatures, which capture the mutational landscape of tumors and are shaped by both genetic factors and environmental exposure, revealed similarities between canine hemangiosarcoma and human angiosarcoma, as reported by Thibodeau and colleagues (36). We analyzed the signatures of trinucleotide mutational frequencies present in golden retriever hemangiosarcomas, and found a strong signature of mutations arising through spontaneous deamination of methylated cytosines in CpG islands, corresponding to COSMIC signature SBS1 and generally associated with aging (ref. 35; Fig. 3; Supplementary Figs. S3–S5). In addition, we see a faint signature not described in COSMIC (Fig. 3). The overall mutational landscape was consistent across all canine hemangiosarcoma tumors, regardless of tumor location or tissue preservation method (Supplementary Figs. S2–S4).

Canine RNA-seq analysis validates exome mutations and extends findings to additional breeds. We validated our exome-sequencing somatic mutation calls using RNA-seq data from a partially overlapping set of dogs ($n = 74$ tumor samples from 73 dogs from 14 breeds, as well as mixed-breed dogs; Supplementary Table S4). Thirteen golden retrievers from the exome cohort with mutations in SMGs had the same tumor location included in the RNA-seq data, with a total of 25 SMG mutations among them. We excluded two frameshift deletion variants from the validation, as they showed evidence of deletion in the pileup data, but also unexpected alternate alleles. Of the remaining 23 variants, we validated 15 (65%) mutations. Of the eight sites which were not validated, one was a nonsense mutation, which may have been subject to nonsense-mediated decay, five had a variant allele fraction (VAF) less than 0.1, and three variants came from samples with tumor purity estimate ($\leq$ 35%) on histologic examination, suggesting that tumor heterogeneity and stromal contamination may be a contributing factor to variants not being replicated (Supplementary Table S5). In the RNA-seq data, four tumor samples from three dogs with variants in the SMGs were from a different tumor site than was included in the exome discovery cohort. In this subset, we were able to detect the mutation discovered in the same individual, but a different tumor location in 4 of 8 (50%) cases. Overall, the group of variants, which we were unable to validate, came from tumor samples with a significantly lower estimated tumor purity on histology ($P_{t\,\text{test}} = 0.04$), but this difference was not significant based on tumor purity estimates from the program ESTIMATE ($P_{t\,\text{test}} = 0.4$; Supplementary Table S5).

The RNA-seq cohort also confirmed that the *TP53* and PI3K pathway mutations were not breed-specific, but were present across different breeds. Excluding the 19 golden retrievers who

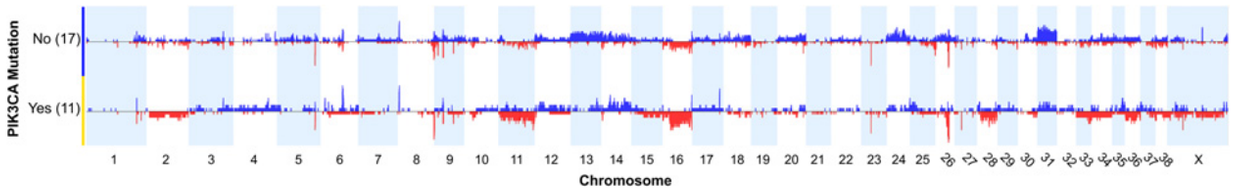

Figure 4.
Comparison of DNA copy number aberration profiles between cases with *PIK3CA* mutation and those without. Blue, copy number gain; red, copy number loss. (Thomas and colleagues, manuscript in preparation; ref. 34)

were also included in the exome cohort, we looked to see whether somatic mutations corresponding to those observed in the exome cohort could be found in other cases, which included Golden Retrievers ($n = 22$), Portuguese water dogs (PWD, $n = 6$), German Shepherd dogs (GSD, $n = 6$), mixed breed dogs ($n = 6$), boxers ($n = 2$), Labrador retrievers (Labs, $n = 2$), Keeshonds ($n = 2$), and other breeds ($n = 8$, one each of American Staffordshire Terrier, Bernese Mountain Dog, Bichon Frise, Briard, Bullmastiff, Gordon setter, Parson's Russell Terrier, and Saluki). We found mutations at the same sites as discovered in the exome cohort in *TP53* ($n = 14$, 26%, 5 breeds), *PIK3CA* ($n = 11$, 20%, 6 breeds), and *PIK3R1* ($n = 4$, 7%, 4 breeds; Supplementary Table S6).

SCNAs

SCNAs in canine hemangiosarcoma recurrently affect known cancer genes. We surveyed SCNAs in genes known to be involved in hemangiosarcoma and angiosarcoma. The genes most recurrently affected by DNA copy number aberrations in the oaCGH data were *VEGFA*, with copy number gain in 19% of cases, *KDR*, gained in 22%, *KIT*, gained in 17%, and the tumor suppressor *CDKN2A/B*, deleted in 22% (Supplementary Table S8). The *MYC* oncogene had copy number gain in 9% of cases. Copy number aberrations in the top significantly mutated genes were relatively rare (Fig. 1A; Supplementary Table S8).

Copy number gains in KDR and losses in AXIN1 are common in both dogs and humans. Comparison of SCNAs in the human data and canine oaCGH data revealed recurrent copy number aberrations in known cancer genes *KDR* and *AXIN1* in both species. Copy number gains in *KDR* occurred in approximately 27% of human samples, and 22% of canine samples. *AXIN1* was lost in 20% of human and 22% of canine samples. In addition, the genes *PTK6*, *ARFRP1*, and *RTEL1* showed copy number loss in 17% of human and canine samples; however, these genes are close together, and also showed copy number gains in a number of canine samples (*PTK6*, 8.7%; *ARFRP1*, 13%; *RTEL1*, 13%; Supplementary Table S9).

SCNA profiles differ among cases with and without PIK3CA mutations. We examined the SCNA profiles of hemangiosarcoma cases with and without *TP53* and *PIK3CA* mutations in the 28 cases with both exome sequencing and oaCGH data. There were no significant differences in the relative frequency of any given CNA between the CNA profiles of cases with and without *TP53* mutations. However, significant differences were detected between cases with *PIK3CA* mutations and those without (Fig. 4), using a two-tailed Fisher exact test and a minimum differential threshold of 25% between the two groups. A region on chromosome 11 at approximately 22.6 Mb, near the *UBE2B* (ubiquitin-conjugating enzyme E2B) gene, was deleted in 4 of 11 cases with *PIK3CA* mutations, and 0 of 17 without ($P < 0.016$). Similarly, the *CDKN2B* gene, located distally on chromosome 11 at 41.2 Mb, was deleted in 4 of 11 cases with *PIK3CA* mutations, and 0 of 17 cases without ($P < 0.016$). A region on chromosome 24 at 21.2 Mb was gained in 7 of 17 cases without *PIK3CA* mutation and 0 of 11 with *PIK3CA* mutation ($P < 0.023$). This region overlaps the antiapoptotic *BCL2L1* gene. Broad copy number gains along the length of chromosome 31 were more frequent in cases without *PIK3CA* mutations compared with those with *PIK3CA* mutations.

Discussion

Detailed molecular profiling of canine hemangiosarcoma has revealed both similarities and differences in the genetic landscape between dogs and humans. In particular, visceral canine hemangiosarcoma showed strong similarities to human angiosarcoma of the viscera and breast. Our findings have important implications for comparative oncology, as the study of canine hemangiosarcoma has the potential to improve our understanding of the pathophysiology of both canine hemangiosarcoma and human angiosarcoma, and to improve treatment and outcomes in both species.

Tumor suppressor *TP53* was the top significantly mutated gene in the canine data. The majority of mutations occurred in the DNA-binding domain, likely causing loss of function (Fig. 2). *TP53* was also the only significantly mutated gene in the human Angiosarcoma Project data, and it has been frequently reported as mutated in targeted sequencing studies of angiosarcoma (25).

We found that the PI3K pathway was commonly mutated in canine hemangiosarcoma. A total of 23 canine tumors (48.9%) had at least one somatic mutation affecting this gene family (Fig. 1A). Tumors with a mutation in the PI3K family tended to have only one mutation in this family. The PI3K pathway is one of the most commonly altered pathways in cancer, playing an important role in signal transduction leading to cell proliferation, survival, differentiation, and regulation of metabolism and immunity (49, 50). *PIK3CA* is an oncogene (51) that has been shown to be mutated in human glioblastoma, breast, gastric, colorectal, lung, and endometrial cancers (52). Ten of the 14 *PIK3CA* mutations in our canine cohort occurred at amino acid position 1047, a mutational hotspot in many human cancers (42). Mutations within this domain have been shown to increase catalytic activity (53).

Of the less frequently mutated SMGs, *PIK3R1* is annotated as a likely driver gene by COSMIC. In addition, variant allele fraction and SIFT scores support a potential role for *RASA1* and *ARPC1A* as driver genes. *RASA1* is a negative regulator of the RAS and MAPK pathways, and plays an important role

in vascular formation (54, 55). Germline *RASA1* mutations can cause capillary malformation—arteriovenous malformation syndrome (56). Somatic mutations in this gene have been found in a subset of human basal cell carcinomas, and expression has been correlated with survival in invasive ductal breast carcinomas and hepatocellular carcinomas (57, 58). *ARPC1A* plays an important role in regulating the actin cytoskeleton, which functions in the migration and invasiveness of pancreatic carcinoma cells (59). There is less support for a causal role for *ORC1* and *ENSCAFG00000017407*; however, it is important to note that the SIFT score does not annotate activating mutations; for example, the hotspot mutations in *PIK3CA* (known to be drivers in many human cancers) are also predicted to be tolerated.

There were also potentially important differences in somatic mutations between the two species. In the human data, mutations in *TP53* and *PIK3CA* tended to be mutually exclusive, while we did not see this pattern in the canine tumors. In addition, *PIK3CA* mutations were exclusively found in breast tumors in the small human dataset, while we found them to be common in cardiac and splenic tumors in dogs. Within the canine visceral tumors, we found fewer mutations in *PIK3CA* in liver tumors. These differences in distribution of *PIK3CA* mutations by tumor location may be due to genetic heterogeneity of the cancer, with tumors in different locations activating the PI3K pathway at different points, or relying on alterations in different pathways to affect an essential protein downstream. It is also possible that this difference is due to the small number of human visceral angiosarcomas currently sequenced, and the small number of liver tumors in the canine cohort.

Another potentially important difference between the two species is that, while copy number gains in *KDR* are common in both species, somatic mutations in this gene were seen in over 20% of human tumors, but in only one canine tumor. As the *KDR* receptor is upstream of the PI3K pathway, it is possible that mutations in either may lead to a similar phenotype. We also saw more copy number gains of *VEGFA* in our canine cohort (19% vs. 0 in the human data), and as *VEGFA* is upstream of *KDR*, this copy number gain may serve a similar role to *KDR* mutations in the canine tumors. In addition, whole genome sequencing will be necessary to determine whether there are common regulatory mutations affecting this gene in canine hemangiosarcoma.

In the human data, mutation rates were significantly different between different tumor locations, with HFNS angiosarcomas having a much higher mutational burden, as reported by Painter and colleagues (46). It is possible that the higher mutational burden in these tumors is due to UV exposure. It would be interesting to compare these findings to canine cutaneous and subcutaneous hemangiosarcomas, which were not included in this study. In the canine visceral hemangiosarcoma, a slight difference was found between mutational burden in heart and splenic tumors. It is possible that the golden retrievers have a lower overall somatic mutation burden than humans, as they likely have a higher germline risk burden, given the high incidence of hemangiosarcoma in the breed. Further studies in dogs will be necessary to determine whether the lower mutation rate is correlated with breed risk, or if in this case it is an artifact of how mutations were called.

Tumors in both dogs and humans were enriched for mutations in protein tyrosine kinases, which are important regulators of cellular growth and division signals and are commonly mutated in cancers. There were also recurrent mutations in the protein tyrosine phosphatase gene family in both species. This may suggest an alternate mechanism of tyrosine kinase overactivation, as protein tyrosine phosphatases deactivate tyrosine kinase signaling by dephosphorylating proteins in opposition to kinase phosphorylation (60). In addition, phospholipase C proteins play a crucial role in cellular signaling pathways by hydrolyzing phosphatidylinositol 4,5-bisphosphate (PIP2) into the second messengers DAG and IP3, passing on signals from receptor tyrosine kinases (61). The canine hemangiosarcomas were enriched for phospholipase C genes, including *PLCG1*, and *PLCG1* mutations were recurrent in the human tumors.

The shared enriched pathways between canine hemangiosarcomas and human angiosarcomas provide insight into disease pathogenesis for both species. Tyrosine kinase inhibitors have been effective against angiosarcoma in the clinic, but tumor heterogeneity and the development of resistance have limited their long-term utility. They have also shown promise against hemangiosarcoma *in vitro* (62), but so far have been less promising in the veterinary clinic (63). Future investigation of the interaction between the many affected pathways will help to determine the potential for combination therapy targeting multiple of these pathways or a common downstream effector to combat resistance.

A recent study in 13 radiation-induced and three spontaneous breast angiosarcomas detected the irradiation signature, as well as the aging signature, and a unique C>T signature (36). The median age of patients in this human cohort was 74.5 years (36). Canine hemangiosarcomas looked very similar, in that we primarily saw the aging signature and low levels of a novel C>T signature. This novel signature bore some resemblance to the signature reported in the human angiosarcomas, including higher levels of C>T mutations at C nucleotides flanked by A-A or A-T; however, there were also differences, such as a high number of mutations flanked by T-G in the dogs, and a low number of these in the human cohort. A larger study will be needed to decipher whether this is a novel angiosarcoma-related signature or whether it represents noise. The lack of the irradiation signature was anticipated as our canine data did not include any tumors secondary to radiotherapy.

We examined copy number changes in canine hemangiosarcoma in genes previously reported to be affected in hemangiosarcoma and angiosarcoma. Most common were copy number gain of *VEGFA* and *KDR*, and loss of *CDKN2A/B*. The *MYC* oncogene, which has been reported amplified in human angiosarcoma and canine hemangiosarcoma, was only rarely gained in our dataset and showed no evidence of high-level amplification. This makes sense, given that it is more common in radiation-induced tumors, which were not present in the canine cohort.

Our data suggest that visceral canine hemangiosarcoma could be developed as a model for primary human angiosarcoma. Detailed molecular characterization of canine hemangiosarcoma revealed many similarities, but also some important differences, between canine hemangiosarcoma and human angiosarcoma. Future work should include analysis of larger cohorts, including recalling all currently available human angiosarcoma data using the same methods, to decipher potential molecular subtypes and to facilitate a more complete comparison between tumors in different locations. An integrated understanding of the interaction between mutations in the many enriched signaling pathways may be useful for

determining treatment strategy; for example, the feasibility of combinations of targeted inhibitors or the prevention of convergent resistance. Our data suggest that clinical trials evaluating therapeutic approaches in dogs with this disease might also inform human medicine.

Disclosure of Potential Conflicts of Interest

J.F. Modiano is a partner (paid consultant) for Veterinary Research Associates, reports receiving a commercial research grant from Boston Scientific, and has ownership interest (including patents) in Half Moon Bay Biotechnology, LLC. No potential conflict of interests were disclosed by the other authors.

Authors' Contributions

Conception and design: C. Painter, M. Breen, J.F. Modiano, I. Elvers, K. Lindblad-Toh

Development of methodology: K. Megquier, J. Turner-Maier, R. Swofford, A.L. Sarver, S. Sakthikumar, K. Lindblad-Toh

Acquisition of data (provided animals, acquired and managed patients, provided facilities, etc.): K. Megquier, R. Swofford, J.-H. Kim, J. Johnson, M. Koltookian, M. Lewellen, M.C. Scott, A.J. Schulte, L. Borst, N. Tonomura, C. Painter, R. Thomas, M. Breen, J.F. Modiano

Analysis and interpretation of data (e.g., statistical analysis, biostatistics, computational analysis): K. Megquier, J. Turner-Maier, J.-H. Kim, A.L. Sarver, C. Wang, S. Sakthikumar, L. Borst, R. Thomas, E.K. Karlsson, J.F. Modiano, I. Elvers, K. Lindblad-Toh

Writing, review, and/or revision of the manuscript: K. Megquier, J.-H. Kim, A.L. Sarver, S. Sakthikumar, M.C. Scott, L. Borst, N. Tonomura, R. Thomas, E.K. Karlsson, M. Breen, J.F. Modiano, I. Elvers, K. Lindblad-Toh

Administrative, technical, or material support (i.e., reporting or organizing data, constructing databases): J. Turner-Maier, R. Swofford, J. Johnson, M.C. Scott, J. Alfoldi

Study supervision: E.K. Karlsson, M. Breen, J.F. Modiano, I. Elvers, K. Lindblad-Toh

Acknowledgments

The authors would like to thank all of the dogs and owners who participated in our research, as well as the veterinarians who collected samples. The results included here include the use of data from The Angiosarcoma Project (https://ascproject.org/), a project of Count Me In (https://joincountmein.org/), downloaded March 2019. We would also like to thank Dr. Scott Moroff, Vice-President and Chief Scientific Officer of Antech Diagnostics, for contributing tumor and paired blood samples to our research. This work was funded by American Kennel Club (AKC) Canine Health Foundation (CHF) grants #422 (to J.F. Modiano), 1131 (to J.F. Modiano), and 1889-G (to J.F. Modiano, M. Breen, K. Lindblad-Toh, E.K. Karlsson), NIH grants R03CA191713 (to J.F. Modiano), P30CA077598 (NIH Comprehensive Cancer Center Support Grant to the Masonic Cancer Center, University of Minnesota), R37CA218570 (to E.K. Karlsson, C. Painter), and R24OD018250 (to E.K. Karlsson), Cancerfonden (K. Lindblad-Toh), National Canine Cancer Foundation (NCCF) grants DM06CO-003 (to J.F. Modiano) and JHK15MN-004 (to J.-H. Kim), and Morris Animal Foundation grant D10CA-501 (to J.F. Modiano, M. Breen, K. Lindblad-Toh). K. Lindblad-Toh is the recipient of a Distinguished Professor award from the Swedish Research Council. I. Elvers is supported by a postdoctoral fellowship from the Swedish Medical Research Council, SSMF. J.F. Modiano is supported by the Alvin and June Perlman Chair in Animal Oncology at the University of Minnesota. M. Breen is supported in part by the Oscar J. Fletcher Distinguished Professorship in Comparative Oncology Genetics at NC State University. A.L. Sarver is supported by NCI R50 CA211249.

The costs of publication of this article were defrayed in part by the payment of page charges. This article must therefore be hereby marked *advertisement* in accordance with 18 U.S.C. Section 1734 solely to indicate this fact.

Received February 22, 2019; revised July 12, 2019; accepted September 25, 2019; published first September 30, 2019.

References

1. Penel N, Marréaud S, Robin YM, Hohenberger P. Angiosarcoma: state of the art and perspectives. Crit Rev Oncol Hematol 2011;80:257–63.
2. Abraham JA, Hornicek FJ, Kaufman AM, Harmon DC, Springfield DS, Raskin KA, et al. Treatment and outcome of 82 patients with angiosarcoma. Ann Surg Oncol 2007;14:1953–67.
3. Florou V, Wilky BA. Current and future directions for angiosarcoma therapy. Curr Treat Options Oncol 2018;19:14.
4. Antonescu C. Malignant vascular tumors—an update. Mod Pathol 2014; 27:S30.
5. Siegel R, Naishadham D, Jemal A. Cancer statistics, 2013. CA Cancer J Clin 2013;63:11–30.
6. Glickman L, Glickman N, Thorpe R. The Golden Retriever Club of America National Health Survey 1998–1999 [Internet]. Available from: https://www.grca.org/wp-content/uploads/2015/08/healthsurvey1-1.pdf.
7. Young RJ, Brown NJ, Reed MW, Hughes D, Woll PJ. Angiosarcoma. Lancet Oncol 2010;11:983–91.
8. Mark RJ, Poen JC, Tran LM, Fu YS, Juillard GF. Angiosarcoma: a report of 67 patients and a review of the literature. Cancer 1996;77:2400–6.
9. Lahat G, Dhuka AR, Hallevi H, Xiao L, Zou C, Smith KD, et al. Angiosarcoma: clinical and molecular insights. Ann Surg 2010;251:1098–106.
10. Stenbäck F. Cellular injury and cell proliferation in skin carcinogenesis by UV light. Oncology 1975;31:61–75.
11. Cioffi A, Reichert S, Antonescu CR, Maki RG. Angiosarcomas and other sarcomas of endothelial origin. Hematol Oncol Clin North Am 2013;27: 975–88.
12. Maddox JC, Evans HL. Angiosarcoma of skin and soft tissue: a study of forty-four cases. Cancer 1981;48:1907–21.
13. Makk L, Creech JL, Whelan JG Jr, Johnson MN. Liver damage and angiosarcoma in vinyl chloride workers. A systematic detection program. JAMA 1974;230:64–8.
14. Centeno JA, Mullick FG, Martinez L, Page NP, Gibb H, Longfellow D, et al. Pathology related to chronic arsenic exposure. Environ Health Perspect 2002;110:883–6.
15. Falk H, Thomas LB, Popper H, Ishak KG. Hepatic angiosarcoma associated with androgenic-anabolic steroids. Lancet 1979;2:1120–3.
16. Calvete O, Martinez P, Garcia-Pavia P, Benitez-Buelga C, Paumard-Hernández B, Fernandez V, et al. A mutation in the POT1 gene is responsible for cardiac angiosarcoma in TP53-negative Li-Fraumeni-like families. Nat Commun 2015;6:8383.
17. Ploegmakers MJ, Pruszczynski M, De Rooy J, Kusters B, Veth RP. Angiosarcoma with malignant peripheral nerve sheath tumour developing in a patient with Klippel–Trénaunay–Weber syndrome. Sarcoma 2005;9: 137–40.
18. Kim JH, Graef AJ, Dickerson EB, Modiano JF. Pathobiology of hemangiosarcoma in dogs: research advances and future perspectives. Vet Sci China 2015;2:388–405.
19. Oksanen A. Haemangiosarcoma in dogs. J Comp Pathol 1978;88: 585–95.
20. Brown NO, Patnaik AK, MacEwen EG. Canine hemangiosarcoma: retrospective analysis of 104 cases. J Am Vet Med Assoc 1985;186:56–8.
21. Withrow SJ, Page RL. Withrow and MacEwen's small animal clinical oncology. Elsevier Health Sciences; 2013.
22. Wendelburg KM, Price LL, Burgess KE, Lyons JA, Lew FH, Berg J. Survival time of dogs with splenic hemangiosarcoma treated by splenectomy with or without adjuvant chemotherapy: 208 cases (2001-2012). J Am Vet Med Assoc 2015;247:393–403.
23. Sorenmo KU, Jeglum KA, Helfand SC. Chemotherapy of canine hemangiosarcoma with doxorubicin and cyclophosphamide. J Vet Intern Med 1993;7:370–6.
24. Tonomura N, Elvers I, Thomas R, Megquier K, Turner-Maier J, Howald C, et al. Genome-wide association study identifies shared risk loci common to two malignancies in golden retrievers. PLoS Genet 2015;11:e1004922.
25. Murali R, Chandramohan R, Möller I, Scholz SL, Berger M, Huberman K, et al. Targeted massively parallel sequencing of angiosarcomas reveals frequent activation of the mitogen activated protein kinase pathway. Oncotarget 2015;6:36041–52.

26. Behjati S, Tarpey PS, Sheldon H, Martincorena I, Van Loo P, Gundem G, et al. Recurrent PTPRB and PLCG1 mutations in angiosarcoma. Nat Genet 2014;46:376–9.
27. Italiano A, Chen CL, Thomas R, Breen M, Bonnet F, Sevenet N, et al. Alterations of the p53 and PIK3CA/AKT/mTOR pathways in angiosarcomas: a pattern distinct from other sarcomas with complex genomics. Cancer 2012;118:5878–87.
28. Wagner MJ, Ravi V, Menter DG, Sood AK. Endothelial cell malignancies: new insights from the laboratory and clinic. NPJ Precision Oncol 2017; 1:11.
29. Je EM, An CH, Yoo NJ, Lee SH. Mutational analysis of PIK3CA, JAK2, BRAF, FOXL2, IDH1, AKT1 and EZH2 oncogenes in sarcomas. APMIS 2012;120: 635–9.
30. Wang G, Wu M, Maloneyhuss MA, Wojcik J, Durham AC, Mason NJ, et al. Actionable mutations in canine hemangiosarcoma. PLoS One 2017;12: e0188667.
31. Mayr B, Zwetkoff S, Schaffner G, Reifinger M. Tumour suppressor gene p53 mutation in a case of haemangiosarcoma of a dog. Acta Vet Hung 2002;50: 157–60.
32. Dickerson EB, Thomas R, Fosmire SP, Lamerato-Kozicki AR, Bianco SR, Wojcieszyn JW, et al. Mutations of phosphatase and tensin homolog deleted from chromosome 10 in canine hemangiosarcoma. Vet Pathol 2005;42:618–32.
33. Abou Asa S, Mori T, Maruo K, Khater A, El-Sawak A, Abd el-Aziz E, et al. Analysis of genomic mutation and immunohistochemistry of platelet-derived growth factor receptors in canine vascular tumours. Vet Comp Oncol 2015;13:237–45.
34. Thomas R, Borst L, Rotroff D, Motsinger-Reif A, Lindblad-Toh K, Modiano JF, et al. Genomic profiling reveals extensive heterogeneity in somatic DNA copy number aberrations of canine hemangiosarcoma. Chromosome Res 2014;22:305–19.
35. Forbes SA, Beare D, Gunasekaran P, Leung K, Bindal N, Boutselakis H, et al. COSMIC: exploring the world's knowledge of somatic mutations in human cancer. Nucleic Acids Res 2015;43:D805–11.
36. Thibodeau BJ, Lavergne V, Dekhne N, Benitez P, Amin M, Ahmed S, et al. Mutational landscape of radiation-associated angiosarcoma of the breast. Oncotarget 2018;9:10042–53.
37. Gorden BH, Kim JH, Sarver AL, Frantz AM, Breen M, Lindblad-Toh K, et al. Identification of three molecular and functional subtypes in canine hemangiosarcoma through gene expression profiling and progenitor cell characterization. Am J Pathol 2014;184:985–95.
38. Borgatti A, Koopmeiners JS, Sarver AL, Winter AL, Stuebner K, Todhunter D, et al. Safe and effective sarcoma therapy through bispecific targeting of EGFR and uPAR. Mol Cancer Ther 2017;16:956–65.
39. Do H, Dobrovic A. Sequence artifacts in DNA from formalin-fixed tissues: causes and strategies for minimization. Clin Chem 2015;61:64–71.
40. Benjamini Y, Speed TP. Summarizing and correcting the GC content bias in high-throughput sequencing. Nucleic Acids Res 2012;40:e72.
41. Kinsella RJ, Kähäri A, Haider S, Zamora J, Proctor G, Spudich G, et al. Ensembl BioMarts: a hub for data retrieval across taxonomic space. Database 2011;2011:bar030.
42. Lawrence MS, Stojanov P, Mermel CH, Robinson JT, Garraway LA, Golub TR, et al. Discovery and saturation analysis of cancer genes across 21 tumour types. Nature 2014;505:495–501.
43. Sondka Z, Bamford S, Cole CG, Ward SA, Dunham I, Forbes SA. The COSMIC Cancer Gene Census: describing genetic dysfunction across all human cancers. Nat Rev Cancer 2018;18:696–705.
44. Ng PC, Henikoff S. SIFT: Predicting amino acid changes that affect protein function. Nucleic Acids Res 2003;31:3812–4.
45. McLaren W, Gil L, Hunt SE, Riat HS, Ritchie GRS, Thormann A, et al. The ensembl variant effect predictor. Genome Biol 2016;17:122.
46. Painter C, Jain E, Dunphy M, Anastasio E, McGillicuddy M, Stoddard R, et al. High mutation burden and response to immune checkpoint inhibitors in angiosarcomas of the scalp and face. In: Proceedings of the Fourth CRI-CIMT-EATI-AACR International Cancer Immunotherapy Conference: Translating Science into Survival; Sept 30–Oct 3, 2018; New York, NY. Philadelphia (PA): AACR; 2019. Abstract nr B085.
47. Kunze K, Spieker T, Gamerdinger U, Nau K, Berger J, Dreyer T, et al. A recurrent activating PLCG1 mutation in cardiac angiosarcomas increases apoptosis resistance and invasiveness of endothelial cells. Cancer Res 2014;74:6173–83.
48. Gonias SL, Karimi-Mostowfi N, Murray SS, Mantuano E, Gilder AS. Expression of LDL receptor-related proteins (LRPs) in common solid malignancies correlates with patient survival. PLoS One 2017;12: e0186649.
49. Fruman DA, Chiu H, Hopkins BD, Bagrodia S, Cantley LC, Abraham RT. The PI3K pathway in human disease. Cell 2017;170:605–35.
50. Cully M, You H, Levine AJ, Mak TW. Beyond PTEN mutations: the PI3K pathway as an integrator of multiple inputs during tumorigenesis. Nat Rev Cancer 2006;6:184–92.
51. Chang HW, Aoki M, Fruman D, Auger KR, Bellacosa A, Tsichlis PN, et al. Transformation of chicken cells by the gene encoding the catalytic subunit of PI 3-kinase. Science 1997;276:1848–50.
52. Samuels Y, Wang Z, Bardelli A, Silliman N, Ptak J, Szabo S, et al. High frequency of mutations of the PIK3CA gene in human cancers. Science 2004;304:554.
53. Hon WC, Berndt A, Williams RL. Regulation of lipid binding underlies the activation mechanism of class IA PI3-kinases. Oncogene 2012;31: 3655–66.
54. Pamonsinlapatham P, Hadj-Slimane R, Lepelletier Y, Allain B, Toccafondi M, Garbay C, et al. p120-Ras GTPase activating protein (RasGAP): a multi-interacting protein in downstream signaling. Biochimie 2009;91:320–8.
55. Henkemeyer M, Rossi DJ, Holmyard DP, Puri MC, Mbamalu G, Harpal K, et al. Vascular system defects and neuronal apoptosis in mice lacking ras GTPase-activating protein. Nature 1995;377:695–701.
56. Eerola I, Boon LM, Mulliken JB, Burrows PE, Dompmartin A, Watanabe S, et al. Capillary malformation-arteriovenous malformation, a new clinical and genetic disorder caused by RASA1 mutations. Am J Hum Genet 2003; 73:1240–9.
57. Liu Y, Liu T, Sun Q, Niu M, Jiang Y, Pang D. Downregulation of Ras GTPase-activating protein 1 is associated with poor survival of breast invasive ductal carcinoma patients. Oncol Rep 2015;33:119–24.
58. Chen YL, Huang WC, Yao HL, Chen PM, Lin PY, Feng FY, et al. Down-regulation of RASA1 is associated with poor prognosis in human hepatocellular carcinoma. Anticancer Res 2017;37:781–5.
59. Laurila E, Savinainen K, Kuuselo R, Karhu R, Kallioniemi A. Characterization of the 7q21-q22 amplicon identifies ARPC1A, a subunit of the Arp2/3 complex, as a regulator of cell migration and invasion in pancreatic cancer. Genes Chromosomes Cancer 2009;48:330–9.
60. Elson A. Stepping out of the shadows: oncogenic and tumor-promoting protein tyrosine phosphatases. Int J Biochem Cell Biol 2018;96:135–47.
61. Kim MJ, Kim E, Ryu SH, Suh PG. The mechanism of phospholipase C-γ1 regulation. Exp Mol Med 2000;32:101.
62. Lyles SE, Milner RJ, Kow K, Salute ME. In vitro effects of the tyrosine kinase inhibitor, masitinib mesylate, on canine hemangiosarcoma cell lines. Vet Comp Oncol 2012;10:223–35.
63. Gardner HL, London CA, Portela RA, Nguyen S, Rosenberg MP, Klein MK, et al. Maintenance therapy with toceranib following doxorubicin-based chemotherapy for canine splenic hemangiosarcoma. BMC Vet Res 2015; 11:131.